Texture Rendering on a Tactile Surface using Extended Elastic Images and Example-Based Audio Cues

Julien Fleureau, Yoan Lefevre, Fabien Danieau,
Philippe Guillotel and Antoine Costes

Technicolor R&I

Abstract. A texture rendering system relying on pseudo-haptic and audio feedback is presented in this paper. While the user touches the texture displayed on a tactile screen, the associated image is deformed according to the contact area and the rubbing motion to simulate pressure. Additionally audio feedback is synthesized in real-time to simulate friction. A novel example-based scheme takes advantage of recorded audio samples of friction between actual textures and a finger at several speeds to synthesize the final output sound. This system can be implemented on any existing tactile screen without any extra mechanical device.

1 Introduction

Texture rendering is an active and challenging field of study where many input and output devices have been proposed. In their survey, Chouvardas et al. classified these textures rendering devices into three categories [3]: mechanical, electrotactile and thermal devices. Mechanical devices stimulates the mechanoreceptors within the skin using mechanical actuators. They include pin-based devices applying pressure, vibrating, ultrasonic and acoustic actuators, and devices based on electrorheological fluids. Electrotactile devices use electric stimulation to activate the mechanoreceptors. A matrix of electrodes is a typical example of such devices. Finally thermal devices provide heat or cool stimuli to the skin.

Another way to simulate texture properties without a specific device is to rely on pseudo-haptic feedback. Lécuyer has shown that various haptic sensations can be induced with visual stimuli [6]. This technique may provide sensations of stiffness, friction, mass of objects or haptic textures. Bump and holes have been simulated by varying the speed of the cursor exploring the texture [7]. The elasticity of a texture was also simulated by a deformation of the image and of the cursor [1]. These two approaches require to explore the texture with a mouse. To make the interaction more natural, Li et al. proposed a similar system embedded on a tablet [8]. The user can feel softness of a surface using a pen or a finger. Punpongsanon et al. developed an augmented reality system where the user touches an actual object while a projector changes the visual appearance of this object [9]. This visual feedback changes the perception of the softness of the object.

Audio stimuli may also modify the perception of texture. Kim et al. shows that the intensity of the sound changes the perception of roughness with or without haptic feedback [5]. The denseness and ruggedness are also affected by this intensity. Even with actual materials such as abrasive papers, sound modifies the perceived roughness [10].

In this work, we present a texture haptic rendering system based on visual and audio pseudo-haptic feedback. It may have applications in the context of e-shopping to virtually touch different materials of interest associated to clothes or furniture for instance. The user by interacting through a standard tactile screen is able to explore the physical properties of the texture, namely stiffness and friction. In line with the approaches mentioned hereinbefore, we rely on visual and audio illusions to generate haptic sensations. The new contributions involved in this latter system are twofolds:

- First, we propose to rely on the paradigm of elastic images introduced in [1], currently limited to punctual pressure contact with a mouse device. We introduce the features of continuous rubbing interaction and non-punctual contact with a finger on a tablet device. To that end, an underlying viscoelastic law and a new contact model are proposed. During the interaction, the texture is visually and dynamically deformed according to the contact area with the finger and rubbing motions.
- Second, a novel example-based audio synthesis process is proposed to render friction properties. It makes use of real audio samples to create a friction sound synchronized to the user's exploratory movement and consistent with the actual texture and rubbing speed.

Both visual deformation and sound synthesis are on-line processes inducing low-computational complexity. In the remaining of this paper these two key components of the global system are further detailed.

2 Pseudo-haptic Rendering

The first aspect of our work deals with a visual mechanism to render pressure interaction when the user is rubbing the texture displayed on the tablet. In the original elastic paradigm [1], the contact duration with the displayed image is assimilated to the amount of "pressure" applied to the associated texture by the end-user. The image is then radially deformed around the contact point with a dedicated heuristic function (see Figure 1) to give the illusion of a true deformation.

However, as it is, this paradigm uniquely addresses static and punctual clicks and the case of a user sliding or rubbing the surface continuously with his finger is not handled. To cope with these limitations, two different enhancements are now introduced. First, a new contact model addresses the problem of natural interaction on a tablet with a finger, and second, a viscoelastic mechanical model is proposed to enable dynamic rubbing motions.

Fig. 1. Left: Deformation obtained from [1]. Right: Deformation obtained with the proposed contact model.

2.1 Contact Model

In [1], the interaction between the user and the image is made by means of a mouse device and the maximum "pressure" is applied at the cursor position.

In the context we address here, the end-user is not interacting with a mouse pointer anymore but rather with his finger. The contact area is not punctual anymore and the whole surface of interaction has thus to be taken into account. In the new contact model, we therefore propose to divide the touched area into two main components (see Figure 2): i) a first component related to the surface right under the contact location, and ii) a second component involving the region right around this contact area.

Fig. 2. Left: Schematic representation of a finger touching the surface. The contact surface is divided into two areas under and around the actual contact zone (respectively green and yellow). Right: The two contact areas represented on an image of a sponge texture.

The maximum amount of "pressure" is now applied on the whole contact surface (and not only a single point) whereas an exponential decrease occurs in the boundary area.

Dedicated heuristic radial functions are also proposed here to quantify the amount of "pressure" applied at a distance d from the contact point after a contact duration t in the two regions defined previously (i.e. $d \in [0, R_{th}]$ and $d \in [R_{th}, R_{max}]$):

$$p^1_{deform}(d,t) = \frac{e^{\frac{5(d-R_{th})}{R_{th}}} - 1}{10} - t \text{ for } d \in [0, R_{th}] \quad (1)$$

$$p^2_{deform}(d,t) = -e^{\frac{-5(d-R_{th})}{R_{max}t}}(t - \frac{1}{50}) \text{ for } d \in [R_{th}, R_{max}] \quad (2)$$

This analytical expression is plotted for various distances and contact durations in Figure 3 and a visual comparison of the contact model from [1] and our is given in Figure 1.

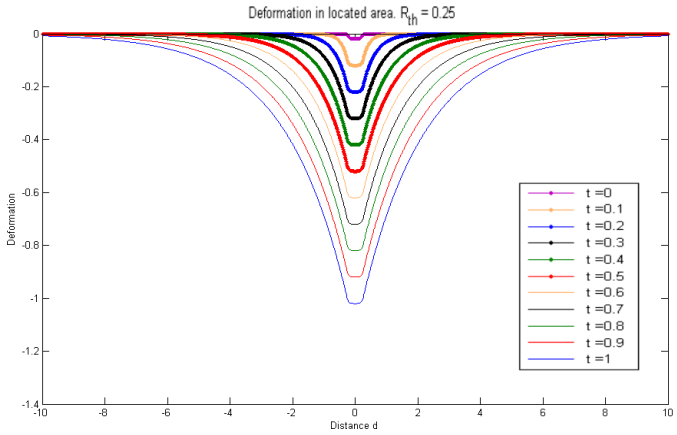

Fig. 3. Plot of the dedicated heuristic radial functions used in the contact model for different contact durations with $R_{max} = 10$ and $R_{th} = 0.25$

2.2 Viscoelastic Model

The original elastic image paradigm [1] is limited to "static" and punctual pressures and it is not designed for sliding or rubbing interactions. The deformation induced by the finger contact is therefore not managed when the end-user moves the contact-point along the texture surface. To cope with this limitation, the textured image is not considered anymore as a 2D deformable object but rather as a 3D grid where each node is associated with one pixel of the texture image. Each vertex is additionally connected to its 4-connected neighborhood.

A purely vertical mechanical viscoelastic model is then associated to this latter 3D grid. It makes successive contacts of the user spatially and temporally consistent on the whole textured image. In this new context, the contact model described in the previous section is not considered anymore as a deformation field but rather as a vertical force field applied to the 3D grid along the z-axis and given as an external input force to the viscoelastic model. The deformation along

the z-axis for each node of the grid is defined by a first order linear differential equation which discrete scheme is given by:

$$P_z[i,j,n] = KE_z[i,j,n] + v\frac{E_z[i,j,n] - E_z[i,j,n-1]}{T_s} \quad (3)$$

The stiffness K and the viscosity v are the 2 parameters involved in the viscoelastic model and:

- $P_z[i,j,n]$ is the "force" at the sample time n, computed with the contact model described hereinbefore (see equations 1 and 2) and applied to the node located at (i,j) in the image plane. At a sample time n, $P_z[i,j,n]$ is maximal under the contact surface.
- $E_z[i,j,n]$ is the deformation / translation along the z-axis. It is noteworthy that $E_z[i,j,n]$ not only depends on the current force $P_z[i,j,n]$ but also on the previous displacement $E_z[i,j,n-1]$.
- T_s is the sampling period.

In steady state (and for a constant input pressure $P_z[i,j,n] = p_z$), the displacement $E_z[i,j,n]$ converges to the value $E_z[i,j,n] = \frac{p_z}{K}$ which is proportional to the force p_z. For transient state (i.e. increase or decrease of the input force), the displacement reaches its steady state value within a time defined by the viscosity parameter ν. In other words, the higher is K, the lower is the final deformation (the stiffer is the texture) and the lower is ν, the faster the texture reaches its steady state. The final deformation thus ensures a time consistency as well as the integration of the user external interaction while preserving low computational loads. Finally, tuning K and ν makes possible to fit different kinds of texture in order to adapt the visual rendering to simulate different "mechanical properties".

2.3 Details of Implementation

The viscoelastic model presented previously can be easily implemented by means of a regular 3D graphic engine. The textured image is used as a regular 2D texture mapped on a 3D regular square grid. Each node of the grid is continuously updated according to equations 1, 2 and 3. A normal is estimated for each node (on the basis of the local neighborhood) at each sample time which enables the use of a light source to do the shadow rendering, thus increasing the realism of the simulation.

3 Example-Based Audio Synthesis

As mentioned hereinbefore, an audio feedback synchronized to exploratory movements improves the realism of the texture rendering and may change the perception of the roughness. In this context, we now propose a method, complementary to the visual feedback, to synthesize a friction sound when the targeted texture

is rubbed by the end-user. The proposed approach is suited for any duration and presents properties which self-adapt with the speed of the rub. Contrarily to [4] and [2] where self-adaptation to speed is proposed on synthesized textures, the proposed method makes use of several real audio recording of the sound generated off-line when touching real samples of the texture of interest at different speed (typically low, medium, high). New sound samples are then synthesized for a given rubbing speed by a combination of the spectral and intensity properties of the initial examples.

The proposed synthesis approach naturally goes through two different steps, namely a learning step and a generation step, that we are going to detail hereafter.

3.1 Learning Step

The initial off-line learning step aimed at capturing the spectral properties as well as the properties of the intensity of the friction sound made when a texture is rubbed at different speeds. These properties will be then re-used in the generation step. To that end, N audio samples s_i are recorded by means of a dedicated setup when a user is rubbing the texture of interest at varying speed v_i. Each signal s_i is first high-pass filtered to remove the baseline which does not embed the high-frequency spectral properties of the texture we are interested in. The remaining part is therefore a centered audio signal, for which spectrum and energy can be computed, and depend on the rubbing speed (see Figure 4).

The spectral properties are captured making use of a regular auto-regressive (AR) model but making use of realistic signals. Such a model is represented by an all-pole infinite Impulse Response filter (IIR) which coefficients v_i are optimized (Yule-Walker equations resolution) so that filtering a white noise with this IIR would result in a new signal with similar spectral properties as the example used for the AR fitting (see Figure 4). The mean power A_i of each temporal sample is also computed to capture the energy properties of the friction sound at each speed.

Eventually, for a given texture, we have N triplets (v_i, F_i, A_i) which characterize its spectral and energy properties at different rubbing speeds. These descriptors are then re-used in the generation step to synthesize the final speed-varying friction sound.

3.2 Generation Step

The synthesis process consists in creating a nth audio sample $y[n]$ consistent with the current rubbing speed $v[n]$ of the end-user as well as with the intrinsic audio properties of the texture. To that end, for each new audio sample to generate at step n:

– N white noises w_i are updated by sampling a new i.i.d. (identically independently distributed) value $w_i[n]$.

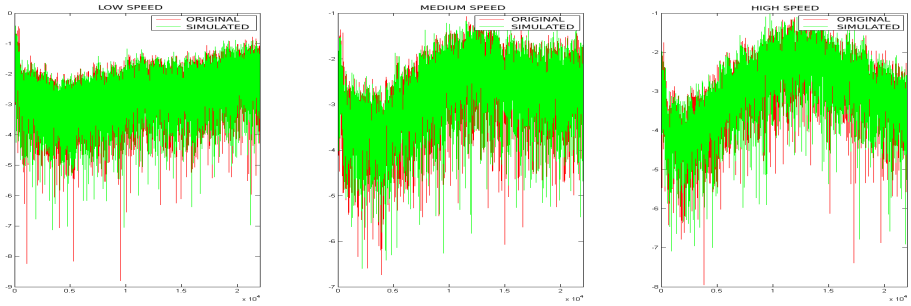

Fig. 4. Original (red) and AR-based estimated (green) spectra of audio samples obtained when recording a user rubbing a sheet of paper at low (left), medium (middle) and high speed (right).

- Each of these N white noises w_i are then filtered through the IIR filter whose coefficients are given by F_i, producing a new associated output $y_i[n]$.
- The 2 consecutive indices a and b such that $v_a \leq v_i \leq v_b$ are then computed.
- Under a linear assumption, a first value $u_0[n]$ is computed by $u_0[n] = \frac{(v_b - v[n])y_a[n] + (v[n] - v_a)y_b[n]}{v_b - v_a}$ which is a weighted value of the signal samples which associated spectra are the closer from the one which should occur at the given speed.
- Still assuming a linear behavior, $u_0[n]$ is finally scaled by a scaling factor $\beta[n] = \frac{(v_b - v[n])A_a + (v[n] - v_a)A_b}{v_b - v_a}$ leading to the final new sample value $u[n] = \beta[n]u_0[n]$.

In the end, the new sample is simply a linear speed-based intensity modulation of a linear speed-based combination of the different spectrally-consistent outputs of the auto-regressive models. Figure 5 sums up the different steps of the generation process.

4 Results & Discussion

We conducted preliminary tests to highlight the advantages as well as the drawbacks of the proposed approach. More precisely, our system has been tested with four different texture samples, namely a sponge ($K = 1.4$ and $\nu = 0.1$), a piece of paper ($K = 7.$ and $\nu = 0.3$), a paper towel ($K = 7.$ and $\nu = 0.3$) and a carpet ($K = 4.$ and $\nu = 0.3$). For each of these materials, examples of audio samples (required for the audio feedback synthesis process) have been captured making use of a Senheiser ME66/K6 microphone on a Zoom R16 recorder. Resulting files are wave formatted file sampled at 44.1 kHz with a 24bits dynamic. The textures were rubbed with the fingertip to produce the sound of friction. Three records per material have been gathered for three different speeds corresponding to slow, medium and fast rubbing speed. All the system has been implemented on the Samsung Galaxy S4 tablet with appropriate images for each visual feedback.

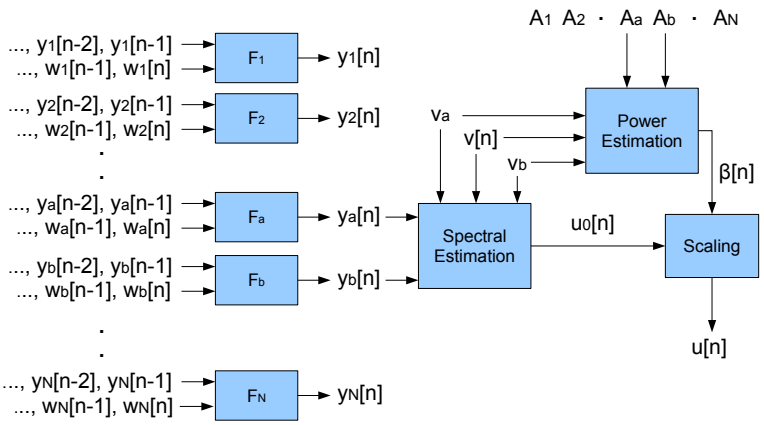

Fig. 5. Block-diagram summing up the different steps involved in the example-based audio synthesis process.

Figure 6 depicts screen captures of the four examples introduced hereinbefore. It is noteworthy to mention that the finger is not represented on the images for illustration purposes, but one should have in mind that the contact areas should be covered by the finger of the end-user. Depending on the consistency of the proposed material with the assumption made in the visual and audio feedback processes, realism and quality of the experience may vary.

First regarding the sponge example, the deformation appears quite realistic because this material has elastic properties which nicely match the viscoelastic model. However, the audio feedback is less convincing because the quite high-frequency content captured by the AR model is not sufficient to render the complexity of the friction sound due to the holes covering the material.

On the contrary, the audio feedback is more realistic for the paper which audio spectrum is more compatible with the assumptions of our audio modeling. The texture deformation looks however mode artificial as the intrinsic mechanical behavior of such a material is poorly represent by an elastic model.

The two last examples fit quite well the underlying modeling assumptions. They both present quite regular surface structures which then produce high-frequency friction sounds compatible with the audio model. Besides, the visual deformation, light for the paper towel, stronger for the carpet, are also realistic because each material are quite well modeled by a viscoelastic law.

The video[1] provided with this paper gives to the reader a more representative idea of the visual and audio behaviors of the whole framework in real conditions. As suggested before, materials presenting mechanical properties close to viscoelastic are obviously better rendered. The sheet of paper for which the elasticity is questionable is therefore poorly deformed whereas the sponge or the carpet provide interesting feedbacks. Similarly, as soon as the friction sounds em-

[1] http://dai.ly/x3pqkwx

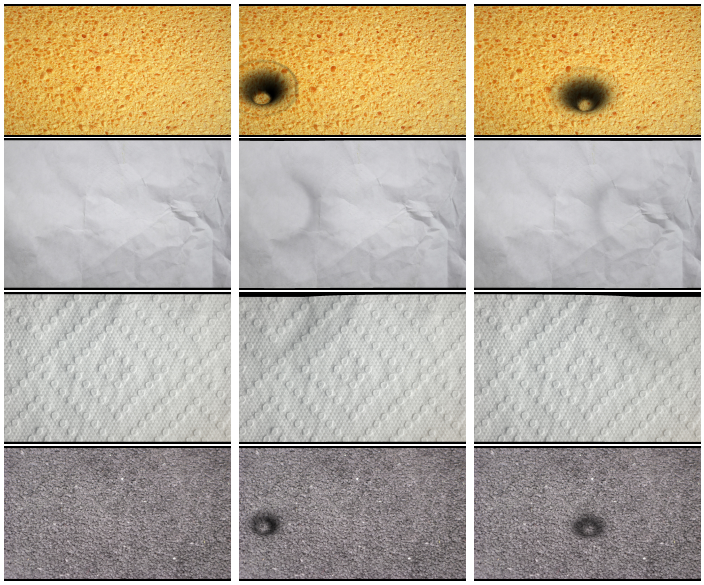

Fig. 6. Examples of textures simulated with the proposed system: sponge, sheet of paper, paper towel and carpet (from top to bottom). The left image is the image of the texture without interaction. The middle image corresponds to a pressure on the left of the screen. The right image is the result of a sliding gesture toward the right.

bed complex patterns induced by meso or macroscopic reliefs, the auto-regressive approach does not provide anymore sufficient degrees of freedom to model the friction sounds. For microscopic reliefs, the speed-varying AR approach is quite relevant and one can especially observe the consistent speed-dependent friction sound variations (in terms of energy and spectrum) obtained on the sheet of paper when changing the rubbing speed. These preliminary tests were necessary to roughly understand the limitations of our systems. More rigorous studies will be conducted to finely characterize the perception of those textures.

5 Conclusion

We have proposed a new framework to render texture properties on a tactile screen without using any extra mechanical device. We relied on the elastic image paradigm and proposed a new contact model based on a viscoelastic law to offer to the end-user a pseudo-haptic visual feedback when he is rubbing or pressing the texture with his finger. Additionally, an example-based audio synthesis methodology has been introduced to render texture-specific friction sounds at different rubbing speeds. First qualitative results have been finally proposed to highlight the advantages as well as the limitations of our approach. Indeed, it seems that elastic materials as well as materials with high-frequency audio signature are better suited for the proposed solution. Future works should now focus

on the generalization of this framework to more complex textures as well as to the setting up of a more quantitative evaluation of the system performances.

References

1. Argelaguet, F., Jáuregui, D.A.G., Marchal, M., Lécuyer, A.: A novel approach for pseudo-haptic textures based on curvature information. In: Haptics: Perception, Devices, Mobility, and Communication, pp. 1–12. Springer (2012)
2. Bianchi, M., Poggiani, M., Serio, A., Bicchi, A.: A novel tactile display for softness and texture rendering in tele-operation tasks. IEEE World Haptics Conference pp. 49–56 (2015)
3. Chouvardas, V., Miliou, A., Hatalis, M.: Tactile displays: Overview and recent advances. Displays 29(3), 185–194 (2008)
4. Culbertson, H., Unwin, J., Kuchenbecker, K.J.: Modeling and rendering realistic textures from unconstrained tool-surface interactions. Haptics, IEEE Transactions on 7(3), 381–393 (2014)
5. Kim, S.C., Kyung, K.U., Kwon, D.S.: The effect of sound on haptic perception. In: EuroHaptics Conference, 2007 and Symposium on Haptic Interfaces for Virtual Environment and Teleoperator Systems. World Haptics 2007. Second Joint. pp. 354–360. IEEE (2007)
6. Lécuyer, A.: Simulating haptic feedback using vision: A survey of research and applications of pseudo-haptic feedback. Presence: Teleoperators and Virtual Environments 18(1), 39–53 (2009)
7. Lécuyer, A., Burkhardt, J., Etienne, L.: Feeling bumps and holes without a haptic interface: the perception of pseudo-haptic textures. In: Proceedings of the SIGCHI conference on Human factors in computing systems. pp. 239–246. ACM (2004)
8. Li, M., Ridzuan, M.B., Sareh, S., Seneviratne, L.D., Dasgupta, P., Althoefer, K.: Pseudo-haptics for rigid tool/soft surface interaction feedback in virtual environments. Mechatronics 24(8), 1092–1100 (2014)
9. Punpongsanon, P., Iwai, D., Sato, K.: Softar: Visually manipulating haptic softness perception in spatial augmented reality. Visualization and Computer Graphics, IEEE Transactions on 21(11), 1279–1288 (2015)
10. Suzuki, Y., Gyoba, J.: Effects of sounds on tactile roughness depend on the congruency between modalities. In: EuroHaptics conference, 2009 and Symposium on Haptic Interfaces for Virtual Environment and Teleoperator Systems. World Haptics 2009. Third Joint. pp. 150–153. IEEE (2009)